

# THE DESIGN OF THE POWER SUPPLY CURRENT LEADS TO A HIGH-TEMPERATURE SUPERCONDUCTING ELECTROMAGNET

GEORGE DUMITRU<sup>1,2</sup>, ALEXANDRU-MIHAIL MOREGA<sup>2,3</sup>, ION DOBRIN<sup>1</sup>, DAN ENACHE<sup>1,2</sup>, CONSTANTIN DUMITRU<sup>1</sup>

**Keywords:** Current leads; Design; Numerical modeling; High temperature superconducting electromagnet; Low temperatures; Heat load.

The paper presents a theoretical and experimental analysis of thermal conditions imposed on the power supply conductor for an HTS YBCO-type high magnetic field electromagnet. For thermal stability during the operation of the electromagnet, it is essential to lower the heat flux from outside the system. The heat from the surrounding environment to the HTS winding is limited by using an adequately sized cryogenic system and the proper design of the current leads. The HTS winding and current leads are cooled with a two-stage GM cryocooler. If the power supply conductor's conductive heat flux exceeds the cryocooler's heat load, the temperature of the HTS winding will increase, and system instability may occur. The power supply conductors are of two types: copper conductors and mixed HTS conductors. This work analyzes HTS conductors and junctions of HTS tape with copper terminals and their contribution to the cryocooler's total heat load. Using HTS conductors reduces Joule heat when current passes through them (approx. 300 A) and the conductive heat flux to the HTS windings. Resistance for various soldering alloys was experimentally evaluated to evaluate the Joule heat of the junctions between HTS conductors and copper terminals.

## 1. INTRODUCTION

The superconducting applications for various devices generating intense magnetic fields require the optimal solution of some issues to ensure the optimal operation of the superconductor winding in stationary conditions. These problems are both electromagnetic and thermal. The structure of a superconducting electromagnet can include LTS materials (low-temperature superconductor) or HTS (high-temperature superconductor) and involves ensuring the cryogenic temperature conditions necessary for stability in the operation of the superconducting windings. These electromagnets made of LTS-type superconducting material (NbTi or Nb<sub>3</sub>Sn) or HTS-type superconducting material (YBCO, BSCCO, MgB<sub>2</sub>, etc.) are cooled with appropriate cryogenic agents (liquid helium for LTS electromagnets and liquid nitrogen for HTS electromagnets). Due to the progress achieved by cryogenics in the last 50 years, an alternative to cryogenic agents consists of using a cryocooler, a closed-cycle heat pump [1,2]. These types of cryocoolers allow for obtaining very low temperatures (up to 2 K) with no use of cryogenic agents, which is an excellent advantage in current conditions because, at this point, helium is a rare and expensive resource. The use of cryocoolers requires a different design compared to a cooling method, which implies the use of cryogenic agents, a design based on solid/solid type thermal conduction cooling.

Since the thermal heat power of these cryocoolers is limited, the superconducting winding conduction-cooled thermal insulation is an essential condition for stability in the operation of the electromagnet. The thermal insulation is mainly ensured by the cryostat in which the superconducting winding is placed. All the mechanical or electrical connections connecting the electromagnet to the outside of the cryostat must be considered to evaluate the thermal flux introduced into the winding through these connections.

The electrical supply system of the electromagnet is provided by a power supply located outside the cryostat, the

current being supplied using two types of conductors (copper and superconductor). These conductors require optimal design to ensure the maximum current supply to obtain the maximum magnetic field. At the same time, they must be designed to allow a minimal heat flux to the superconducting winding.

Obtaining intense magnetic fields (> 2 T), so necessary in many nuclear physics applications (particle accelerators, particle detectors, etc.), led to the replacement of the conventional electromagnets with superconducting electromagnets, generally LTS type, cooled with liquid helium (4.2 K) [3–6].

Recently, there has been a strong tendency to replace these conventional electromagnets with HTS type [7–10] due to the possibility of obtaining very high magnetic fields, which have electrical and magnetic properties superior to the LTS type electromagnets. This category also includes the HTS electromagnets with a dipolar magnetic field, with the maximum magnetic flux density generated higher than 5 T [11,12].

In this paper, the sizing and thermal regime of the HTS conductors are analyzed, which is an important part of the electrical supply system of the superconducting electromagnet generating a uniform magnetic field with the magnetic flux density of 5 T, designed, and realized in the Applied Superconductivity Laboratory of ICPE-CA, Bucharest [11].

The copper conductors that connect the external power supply to the superconducting winding of the electromagnet through the HTS conductors analyzed here were designed and analyzed in previous works [12].

## 2. MAGNET SYSTEM DESCRIPTION

Figure 1 shows the schematic view of the HTS magnet system. Which comprise the cryostat of the magnet (1), the superior flange of the cryostat (2), the cryocooler (3) type Gifford- McMahon [14], the outer copper connectors (4) to the power supply, the copper leads (5), the copper flange (6) connected to the 1st stage of the cryocooler, the HTS leads

<sup>1</sup> National Institute for Research and Development in Electrical Engineering ICPE-CA, 313 Splaiul Unirii, District 3, 030138, Bucharest, Romania, E-mails: george.dumitru@icpe-ca.ro, dan.enache@icpe-ca.ro, ion.dobrin@icpe-ca.ro, constantin.dumitru@icpe-ca.ro

<sup>2</sup> The Doctoral School of Electrical Engineering, 313 Splaiul Independentei, District 6, 060042, Bucharest, Romania, E-mails: george.dumitru@icpe-ca.ro, amm@iem.pub.ro, dan.enache@icpe-ca.ro

<sup>3</sup> "Gh. Mihoc – C. Iacob" Institute of Statistical Mathematics and Applied Mathematics, Romanian Academy, E-mail: amm@iem.pub.ro

(7) connected to the HTS magnet (8) who is protected from thermal radiation by the thermal shield (9) and cooled by conduction through the copper links (10) who are connected to the 2<sup>nd</sup> stage of the cryocooler.

The cryostat is vacuumed to a low pressure of a minimum of  $10^{-5}$  mbar to reduce/eliminate the thermal losses by residual gas convection. The HTS electromagnet is designed and executed as a split coil electromagnet with two series-connected sections to generate a high magnetic field (5 T) in the central (axial) area. The design and the execution of the electromagnet were detailed in previous works [14, 15]. The HTS electromagnet is cooled by conduction using a closed-cycle G-M Cryocooler from SHI Cryogenics [13]. The cryocooler model is RDK 415D and has two cooling stages: 1st stage has a 50 K temperature, and the second stage reaches the final temperature of 4.2 K. The first stage of the cold head is thermally connected to the copper flange and the thermal shield, protecting the HTS magnet against the thermal radiation from the cryostat and preventing it from heating the electromagnet.

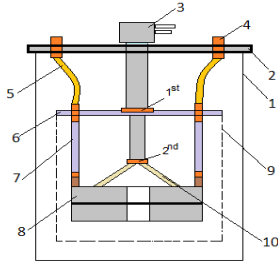


Fig. 1 – Schematic view of the HTS electromagnet assembly.

## 2.1. ELECTRICAL SUPPLY MIXED CONDUCTORS

The electric power supply conductors for the HTS superconductor winding have two types of inserted conductors in their components. Thus, the current from the power supply is brought to the superconducting winding through a copper conductor and an HTS conductor. This setup is necessary to limit the thermal heat flux to the HTS superconducting winding.

The design of the copper conductors and their contribution to the amount of heat power brought from the external environment of the cryostat to the inside was carried out in a previous work [12].

The HTS connectors that connect the copper conductors and the superconducting winding of the HTS magnet will be analyzed. They aim to ensure intense currents (300-400 A) supply without the Joule effect and minimum heat flux to the HTS winding. The HTS current lead is an electrical conductor with a complex structure consisting of an external protective shield, the HTS conductor type, and two copper terminals. The two copper terminals ensure electrical connection with the copper conductor, respectively, with the superconducting electromagnet's power terminals. The HTS conductors are made with YBCO tape, and the properties are presented in Table 1.

Table 1  
HTS conductor characteristics [16]

No.	Quantity	Value
1	Superconductor	YBCO
2	Shape	Tape
3	Width [mm]	12
4	Thickness [mm]	0.11
5	Critical current $I_c$ [A] @ 77 K	300
6	Minimum bending diameter [mm]	11

The YBCO-type HTS conductor presented in Table 1 is manufactured by Superpower Inc. [16] in a multilayer technique, the superconducting layer having only 1  $\mu\text{m}$  thickness. This superconducting tape has a multilayer complex structure (Fig. 2), the superconducting layer having just 1  $\mu\text{m}$  thickness.

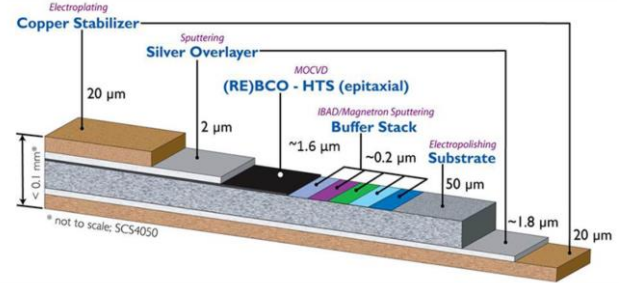


Fig. 2 – SuperPower HTS tape structure [16].

## 2.2. NUMERICAL MODELING

A numerical model was created using the finite element technique to evaluate the temperature profile of the HTS current leads. For this, a geometrical model consisting of a copper terminal, HTS tape, and the external shield is shown in Fig. 3.

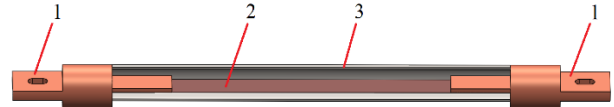


Fig. 3 – Geometric model of HTS conductor: 1 – copper terminal; 2 – HTS tape; 3 – protective shield.

The discretization network, which consists of 47345 elements, is presented in Fig. 4.

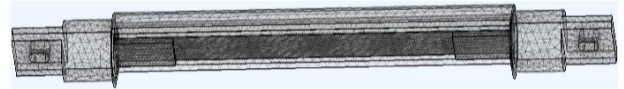


Fig. 4 – HTS current lead discretization network.

Two mathematical models were used for this heterogeneous HT superconductor / normal conductor. The first model is used for the electric current flow to evaluate the Joule heating:

$$\nabla \cdot (\sigma \nabla V) = 0. \quad (1)$$

where  $\sigma$  [S/m] is the electric conductivity of the copper terminals, and  $V$  [V] is the electric potential. The HT domain is discarded because it is assumed to be superconducting with no resistive losses. So, (1) is solved for each copper terminal: problem P1, left terminal in Fig. 3, and problem P2, for the right terminal in Fig. 3. The BCs are as follows:

- P1 – inlet current density ( $J_n$  corresponding to the stationary current  $I = 300$  A through the copper terminals) for the current inlet, ground for the exit, and electric insulation elsewhere.
- P2 – inlet current density at the upstream current cross-section (copies the exit current density in P1) ground for the exit cross-section, and electric insulation elsewhere.

The two problems are coupled through the voltage BCs. This approach is implemented conveniently by setting a periodicity

condition: the voltage of the upstream section in P2 equals the voltage (floating) of the downstream section in P1. These BCs map the current density distribution from the left lead's cross-section exit to the right lead's entrance cross-section.

The second model concerns the pending heat transfer problem, particularly in the two copper terminals:

$$\nabla(\nabla T) + \frac{\dot{Q}}{k} = 0, \quad (2)$$

where  $T$  [K] is the temperature,  $\dot{Q} = \mathbf{J} \cdot \mathbf{E}$  [W/m<sup>3</sup>] is Joule heat generation rate,  $k$  [W/(m·K)] is the thermal conductivity of the material, and  $\mathbf{E}$  is the electric field. Thermal conductivity values for shield materials used in this model are presented in Table 2. Figure 5 depicts the thermal conductivities as a function of temperature.

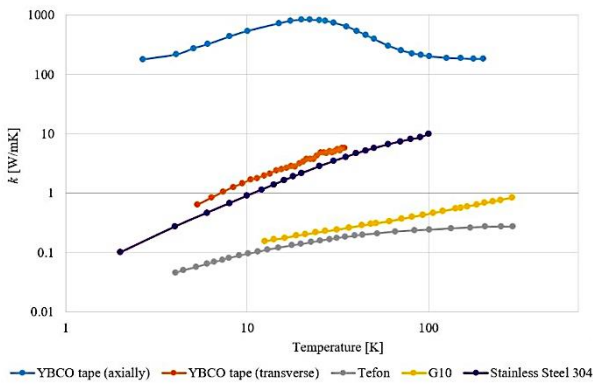


Fig. 5 – Thermal conductivities for materials used [17-19].

Table 2  
Thermal conductivities [17-19]

Material type	$k(T)$ [W/m·K] for the range 4.2 – 50 K
YBCO tape (axially)	180 – 837
YBCO tape (transverse)	0.22 – 5.67
Stainless steel	0.272 – 5.730
Teflon (PTFE)	0.045 – 0.21
G10	0.073 – 0.306

Unlike the electric field problem, the HTS tape and the shield are part of the computational domain (without internal heat sources). The space between them is discarded and does not participate in the heat transfer – a void with neither conduction heat transfer nor radiative heat transfer between its faces. The boundary conditions are shown in Fig. 6.

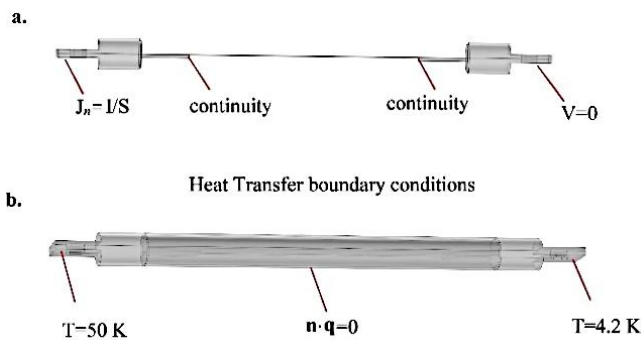


Fig. 6 – HTS current leads model: a) Electric current boundary conditions; b) Heat transfer boundary conditions.

The terminal at the right is connected to the cryocooler, and its temperature is set to 4.2 K. The initial temperature of the mixed HTS conductor assembly is  $T = 50$  K.

### 2.3. NUMERICAL SIMULATION RESULTS

Numerical modeling aimed to find the optimal solution to minimize the thermal flow in HTS current leads. For this, several materials with different thicknesses and thermal conductivities were used for the HTS current leads shield.

The materials selected for this model and the corresponding thicknesses are presented in Table 3.

Table 3  
Materials used for the shield of the HTS conductor

No.	Material type	Thickness [mm]
1	Stainless steel	0.5
2	Stainless steel	1
3	Teflon (PTFE)	3
4	G10	3

The two terminals of the HTS current leads are connected to the two cooling stages of a cryocooler, the first at 50 K, and the second at 4.2 K. The HTS supply current conductor was set to 300 A dc.

The temperature profile of the HTS conductor assembly is presented in Fig. 7.



Fig. 7 – Temperature profile for HTS conductor with 1 mm stainless steel shield (in the range of 4.2 K (indigo) to 50 K (white)).

The conductive heat rate found through numerical modeling for HTS conductors with different materials for the shield is presented in Table 4.

Table 4  
Conductive heat flux for HTS current leads

Shield material type	Thickness [mm]	Conductive heat rate [mW]
Stainless steel	0.5	87.01
Stainless steel	1	122.61
Teflon (PTFE)	3	103.79
G10	3	104.58

As an obvious conclusion, using 0.5 mm thickness stainless steel 304 is the best shield material with the lowest heat transfer power.

### 3. JUNCTION CONTACT RESISTANCE

To estimate the total heat load of the HTS electromagnet due to the current supply conductors, we need to evaluate the Joule heat generated by the electrical contact between the HTS tape and copper terminals. An experimental study of the soldering junction between two HTS tapes must be performed for this.

The junction between two superconducting types can be achieved in two ways: the first method consists of heating the soldering alloy and the area to be soldered by the electromagnetic induction method [20], and the second and most common method consists of using a resistive heating plate assembly at a desired temperature [21].

To achieve the junction of the HTS types, a temperature-controlled plate was designed and made (Fig. 8). The temperature control of the plate was ensured using a temperature controller model, OMRON E5CC. The temperature range of the soldering plate can be set from 50 °C up to 300 °C.

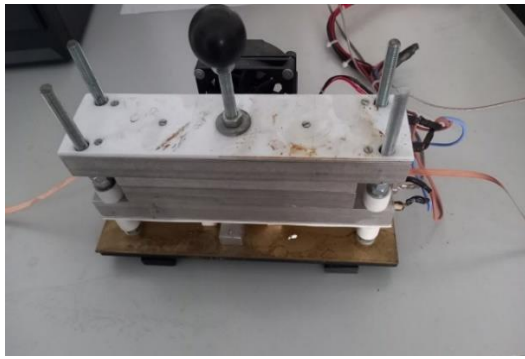


Fig. 8 – Temperature-controlled device for soldering.

To measure the junction electric resistance of the HTS superconducting tape, several samples were made using different soldering alloys to establish the optimal parameters for this type of junction. The main goal is to achieve the minimum electrical resistance of the tape junction to minimize the Joule heating. The junction of the superconducting tapes was made for an overlap of 100 mm length at a pressure of 100 kPa. Figure 9 shows two SuperPower HTS superconducting tapes 12 mm wide, soldered together for an overlap of 100 mm.

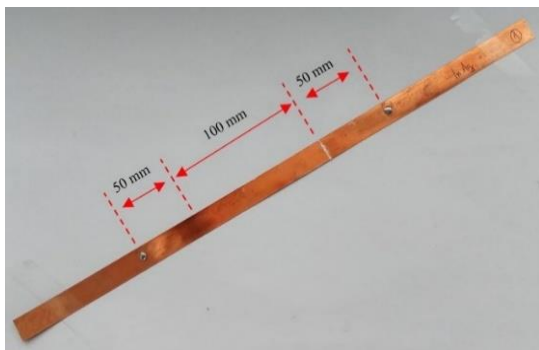


Fig. 9 – Junction of two HTS types soldered on 100 mm overlap length.

Several junctions were made using 12 mm wide superconducting HTS type for 100 mm overlap. For these, different soldering alloys produced by Indium Corporation were used [22]. Their main characteristics are presented in Table 5.

Table 5  
Soldering alloy parameters [22]

Alloy (%)	Melting temperature [K]	Density [g/cm <sup>3</sup> ]	Thermal conductivity [W/cm·K]
52 In / 48 Sn	391	7.30	0.34
60 In / 40 Pb	454	8.52	0.29
97 In / 3 Ag	416	7.38	0.73
100 In	430	7.31	24
63 Sn / 37 Pb	456	0.5	0.5

After soldering all the HTS tapes at controlled temperature and pressure, the samples were immersed in liquid nitrogen (77 K), and electrical measurements were made using a 0 to 300 A programmable DC power supply. The voltage drop across the HTS junctions was measured with a Keithley 2182 nanovoltmeter to evaluate the electrical resistance of each sample.

Figure 10 presents the measurement results of the soldered joints. The lowest resistance calculated was 15,3 nΩ ±2,629 % for 97 % In / 3 % Ag alloy.

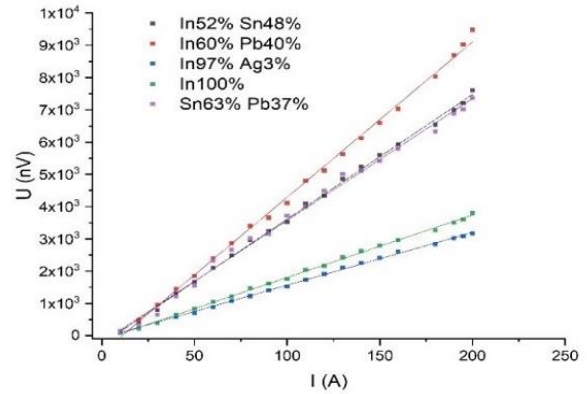


Fig. 10 – The U-I characteristic of the junction for several types of soldering alloys.

#### 4. CRYOGENIC COOLING SYSTEM

The cryogenic cooling system of the HTS electromagnet is based on a closed-cycle G-M cryocooler system from SHI Cryogenics [13], which works with helium gas and has two cooling stages, the first stage has a temperature of 50 K, and the second stage can reach the final temperature of 4.2 K. The first stage of the cryocooler is thermally anchored to the electromagnet’s thermal shield. The second stage is thermally attached to the electromagnet housing, pumping out the heat of the HTS coils by conduction and lowering their temperature to values close to 4.2 K. Figure 11 presents a schematic view of the cold head.

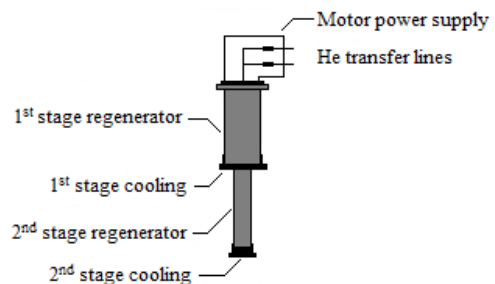


Fig. 11 – The cryogenic cooling system consists of a two-stage cooling unit.

Table 6 summarizes the functional characteristics of the RDK 415D cryocooler from SHI Cryogenics [13].

Table 6  
RDK 415 D model characteristics [13]

No.	Characteristic	Value
1	1 <sup>st</sup> stage temperature	50 K
2	2 <sup>nd</sup> stage temperature	4.2 K
3	1 <sup>st</sup> stage thermal power	50 W
4	2 <sup>nd</sup> stage thermal power	1.5 W

#### 5. CONCLUSIONS

The work performed here presented the structure of the electrical power supply conductor system of an HTS superconducting electromagnet and the evaluation of the operating conditions and thermal parameters of operation for the supply conductors, especially the HTS superconducting conductors.

For the temperature stability operation (in stationary conditions) of the superconducting coils of the HTS

electromagnet, it is essential to minimize the conductive heat flux to as low as possible. Thus, the heat flux from the outside to the HTS winding is limited by using a properly sized cryogenic system and by the appropriate sizing of the supply conductors.

HTS conductors in this application have two reasons: reducing the Joule heat when current passes through them (approx. 300 A) and keeping the conductive heat flux to the HTS winding as low as possible.

A constructive solution was chosen by using a 12 mm wide HTS superconducting tape with 0.11 mm thickness. The source of Joule heating has two components: the copper terminals and HTS junctions with the copper terminals. The HTS junctions were investigated from the resistance point of view for various soldering alloys. The alloy with the lowest resistance is 97 % In / 3 % Ag, with an electrical resistance at 77 K of 15.3 nΩ.

The temperature profile and the heat produced by the mixed HTS conductors were carried out using FEM numerical modeling. Several constructive types were analyzed using different shield materials, finding that 304 stainless steel is the optimal choice.

The conclusions of the modeling were: the heat power transmitted between 50 K and 4.2 K is 87.01 mW, and the Joule power due to the soldered junctions is 0.8 mW.

The total heat to the HTS winding of the electromagnet, produced and conducted using HTS mixed conductors analyzed in this work, is 174.82 mW, which is well below the power of the second cooling stage of the cryocooler of 1.5 W for a temperature of 4.2 K. So, the HTS conductors supply system with the dimensional and functional characteristics obtained in this analysis, are suitable for obtaining a steady-state operation of the HTS winding of the electromagnet.

#### ACKNOWLEDGEMENTS

The authors acknowledge the funding of this work through the financing of project 42N-PN23140101/2023, supported by the Romanian Ministry of Research, Digitization, and Innovation (MCDI).

*Received on 10 October 2023*

#### REFERENCES

1. R. Radebaugh, *Refrigeration for superconductors*, Cryogenic Technologies Group, National Institute of Standards and Technology, Boulder, CO 80305 USA; Proc. of the IEEE, **92**, 10 (2004).
2. R. Radebaugh, *Review of refrigeration methods*, [https://trc.nist.gov/cryogenics/Papers/Review/2020-Review\\_of\\_Refrigeration\\_Methods.pdf](https://trc.nist.gov/cryogenics/Papers/Review/2020-Review_of_Refrigeration_Methods.pdf)
3. H. Maeda, Y. Yanagisawa, *Future prospects for NMR magnets: A perspective*, Journal of Magnetic Resonance, **306**, pp. 80–85 (2019).
4. P. Schmuser, *Superconducting magnets for particle accelerators*, Rep. Prog. Phys. **54**, 683 (1991).
5. L. Rossi, L. Bottura, *Superconducting magnets for particle accelerators*, Reviews of Accelerator Science and Technology, **5**, pp. 51–89 (2012).
6. I. Dobrin et al., *High-temperature superconductor dipolar magnet for high magnetic field generation – design and fabrication elements*, 10<sup>th</sup> International Symposium on Advanced Topics in Electrical Engineering (ATEE), Bucharest, Romania, 2017, pp. 201–205.
7. M. Daibo, S. Fujita, M. Haraguchi, Y. Iijima, M. Itoh and T. Saitoh, *Development of a 5 T 2G HTS magnet with a 20-cm-diameter Bore*, IEEE Transactions on Applied Superconductivity, **23**, 3, pp. 4602004–4602004 (2013), Art no. 4602004.
8. Dobrin, A.M. Morega, A. Nedelcu and M. Morega, *Design and fabrication of a 5 T NbTi solenoid magnet cooled by a closed-cycle G-M cryocooler*, International Symposium on Advanced Topics in Electrical Engineering (ATEE), Bucharest, Romania, 2013, pp. 1–4.
9. C.K. Yang et al., *Design, Fabrication, and Performance Tests of a HTS Superconducting Dipole Magnet*, in IEEE Transactions on Applied Superconductivity, **22**, 3, pp. 4000804–4000804 (2012).
10. H.W. Weijers et al., *High field magnets with HTS conductors*, in IEEE Transactions on Applied Superconductivity, **20**, 3, pp. 576–582 (2010).
11. I. Dobrin, A. Cernikov, S. Kulikov, A. Buzdavin, O. Culicov, A.M. Morega, A. Nedelcu, M. Morega, I. Popovici, and A. Dobrin, *A 4 T HTS magnetic field generator, conduction-cooled, for neutron physics spectrometry*, IEEE Transactions on Applied Superconductivity, **26**, 3 (2016).
12. G. Dumitru, A. Morega, I. Dobrin, D. Enache, A. Nedelcu, *Analysis of the thermal and electrical parameters of the supply system of an HTS superconducting electromagnet*, International Conference and Exposition on Electrical and Power Engineering (EPE), 2022
13. SHI Cryogenics Group, <https://www.shicryogenics.com/products/cryocoolers/>
14. G. Dumitru, I. Dobrin, D. Enache, *Design of a HTS superconducting electromagnet for intense and uniform high magnetic field* (translated from Romanian), APME — Electric Machines, Materials and Drives – Present and Trends, **18**, 1, pp. 125–135 (2022).
15. G. Dumitru, A. Morega, I. Dobrin, D. Enache, A. Dobre, C. Dumitru, *Thermal influence of a variable temperature insert on the high-temperature superconductor coils of a conduction cooled high magnetic field generator*, The 13<sup>th</sup> International Symposium on Advanced Topics in Electrical Engineering March 23–25, 2023, Bucharest, Romania.
16. Superpower Inc., <https://www.superpower-inc.com/specification.aspx>.
17. N. Bagrets, W. Goldacher, S. I. Schlachter, C. Barth, Klaus-Peter Weiss, *Thermal properties of 2G coated conductor cable materials*, Cryogenics, **61**, pp. 8–14 (2014).
18. Y. Iwasa, *Case Studies in Superconducting Magnets: Design and Operational Issues*, Springer Science + Business Media, LLC, 2009.
19. M. Bonura, C. Senatore, *Transverse Thermal Conductivity of REBCO Coated Conductors*, IEEE Transactions on Applied Superconductivity, **25**, 3 (2015).
20. D. Marian, M. Eva, P. Marcela, P. Marian, F. Lubomir, G. Peter, J. Igor, M. Jozef și G. Fedor, *Induction soldering of coated conductor high-temperature superconducting tapes with lead-free solder alloys*, IEEE Transactions on Applied Superconductivity, **28**, 4 (2018).
21. J.S. Murtoimäki, G. Kirby, J. Van Nugteren, P.-A. Contat, O.S. De Frutos, J. Fleiter, F.-O. Pincot, G. de Rijk, L. Rossi, J. Ruuskanen, A. Stenvall și F.J. Wolf, *10 kA joints for multi-tape HTS Cables*, Magnet Technology, Amsterdam, N., 2017.
22. Indium Corporation, <https://www.indium.com>.